PHILOSOPHICAL TRANSACTIONS OF THE ROYAL SOCIETY A
MATHEMATICAL, PHYSICAL & ENGINEERING SCIENCES

Marginally separated flows in dilute and dense gases

Alfred Kluwick

Phil. Trans. R. Soc. Lond. A 2000 **358**, 3169-3192
doi: 10.1098/rsta.2000.0703

10.1098/rsta.2000.0703

Marginally separated flows in dilute and dense gases

By Alfred Kluwick

Institute of Fluid Dynamics and Heat Transfer, Vienna University of Technology, Karlsplatz 13, A-1040 Wien, Austria

The paper concentrates on flow effects which occur if a two-dimensional almost separated boundary layer is disturbed by a three-dimensional surface-mounted obstacle. In addition to dilute gases which satisfy the perfect gas law, dense gases are also considered. These have the distinguishing feature that the fundamental gasdynamic derivative Γ can change sign. As a result, rarefaction shocks may form which, in the case of dilute gases, are ruled out by the second law of thermodynamics. More important in the present context, however, it is found that the non-monotonous Mach number variation during isotropic compression associated with the unusual Γ-behaviour represents a new non-classical mechanism for the formation of marginally separated flows.

Keywords: laminar boundary layers; boundary-layer separation; marginal separation; dense gases

1. Introduction

The properties of a two-dimensional, incompressible laminar boundary layer near a point of vanishing skin friction have been investigated, first by Prandtl (1938) and in a more systematic manner by Goldstein (1948). These investigations showed that the wall shear-stress distribution may exhibit a square-root singularity and it has been presumed ever since that this Goldstein singularity represents an impasse as far as classical boundary-layer theory is concerned. A typical example is provided by the linearly retarded flow past a thin flat plate studied by Howarth (1938) and Hartree (1939), who found that the solution of the boundary-layer equations could not be extended beyond the point of zero wall shear which in part stimulated Goldstein's work. Further evidence for this point of view has been provided by Ruban (1981*a*, *b*) and Stewartson *et al.* (1982). In addition, these authors showed that there exists yet another type of singular solutions of the boundary-layer equations, which have the remarkable property that the wall shear vanishes at some point characterized by a value $\tilde{x}_0$ of the coordinate in the streamwise direction, say, but immediately recovers so that it can be continued further downstream. Solutions of this type are relevant, for example, to flows past slender aerofoils at small angles of attack. Owing to the large streamline curvature in the nose region, the fluid overexpands as it accelerates from stagnation conditions to flow along the upper surface and thus has to be recompressed further downstream. This in turn causes the wall shear to decrease eventually and if the angle of attack is just right it vanishes in a single point but remains positive elsewhere.

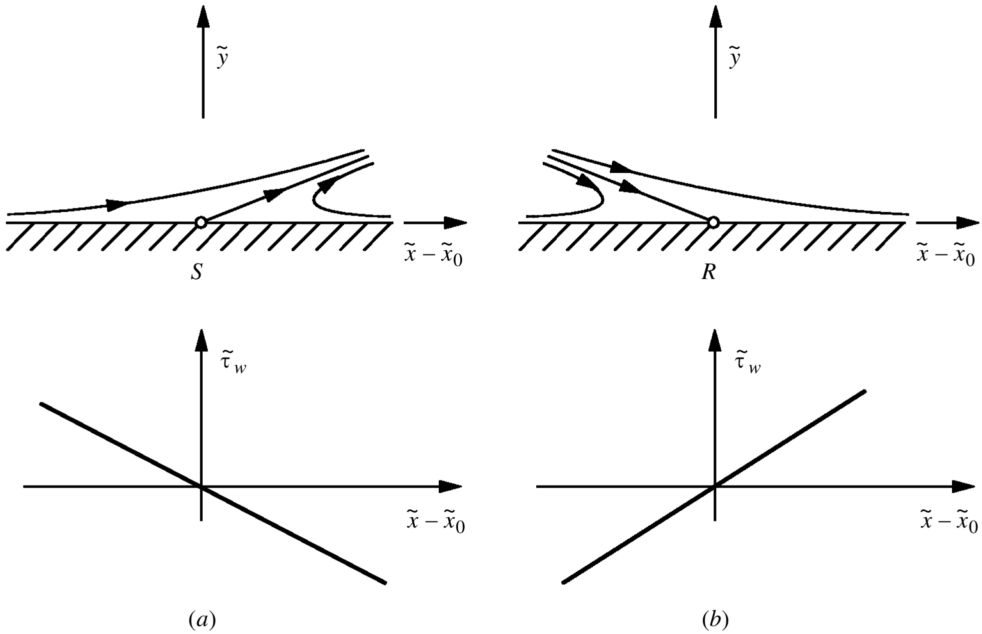

Figure 1. Streamline pattern and wall shear-stress distribution near a separation point (*a*), reattachment point (*b*).

As shown in Ruban (1981*a*, *b*) and Stewartson *et al.* (1982), the properties of the boundary layer in the vicinity of this point can be studied rigorously using asymptotic techniques. The existence of such a solution and its basic features can be inferred, however, from more simple considerations. To this end we note that local solutions of the full Navier–Stokes equations which describe the flow behaviour in the neighbourhood of a separation or reattachment point have been obtained, among others, by Oswatitsch (1958). The resulting streamline patterns and wall shear stress distributions are sketched in figure 1. As observed by Kluwick *et al.* (1984), these local solutions of the Navier–Stokes equations also satisfy the boundary-layer equations to leading order. In contrast to the Navier–Stokes equations, however, the boundary-layer equations do not contain second-order derivations with respect to $\tilde{x}$. Therefore, if we cut the diagrams displayed in figure 1 which correspond to regular separation and reattachment along the vertical axes and interchange the inner and outer parts, we obtain new local solutions of the boundary-layer equations (which, of course, are no longer local solutions of the Navier–Stokes equations) (figure 2). Here we are interested in the results shown on the right-hand side which represent the case of marginal separation. On physical grounds one expects that this specific solution of the boundary-layer equations is embedded in a one-parameter family of solutions which describes the transition from completely smooth wall shear stress distributions if a suitable chosen controlling parameter k (the angle of attack in the example of a slender aerofoil) is smaller than a critical value k_0 to wall shear stress distributions which terminate in the form of a Goldstein singularity if $k > k_0$ (figure 3). In the limit $k-k_0 \to 0+$ the strength of the Goldstein singularity then becomes arbitrarily small, and, as shown by Ruban (1981*b*) and Stewartson *et al.* (1982), the asymptotically

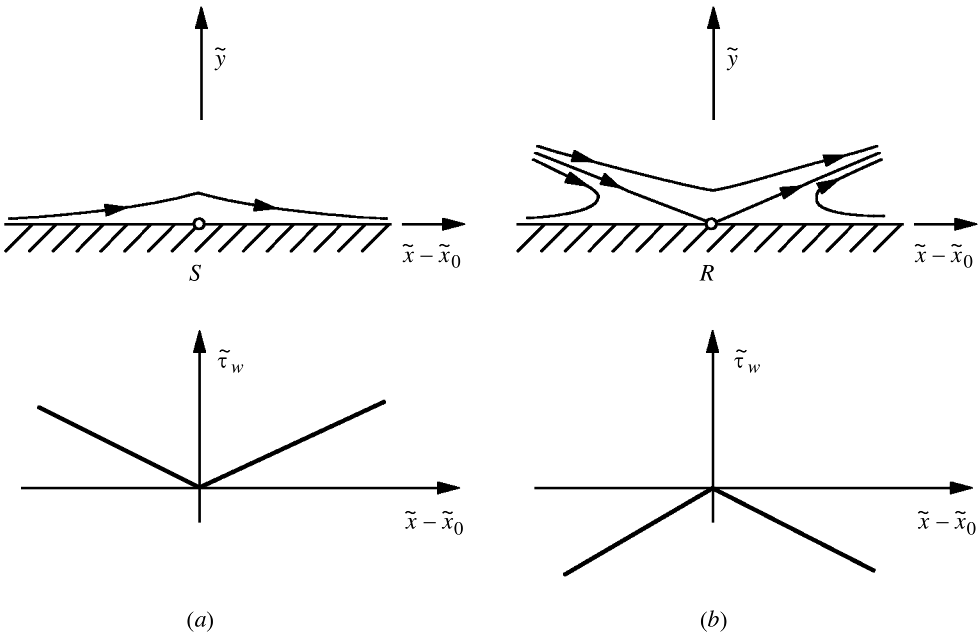

Figure 2. Streamline pattern and wall shear stress distribution corresponding to marginal separation (a), marginal reattachment (b).

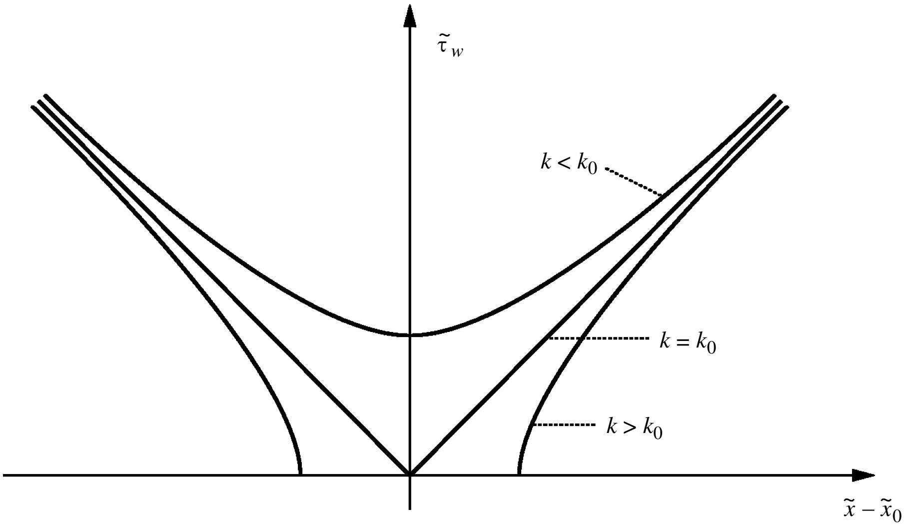

Figure 3. Wall shear stress distributions for various values of the controlling parameter k.

short gap where classical boundary-layer theory fails can be bridged by taking into account the interaction between the boundary layer and the external inviscid flow.

The theory of marginally separated flows, therefore, provides another example where the formation of a separation singularity can be avoided successfully by means of an interaction strategy. In contrast to triple deck theory, however, it is not the rapid change of the boundary conditions which forces an initially firmly attached

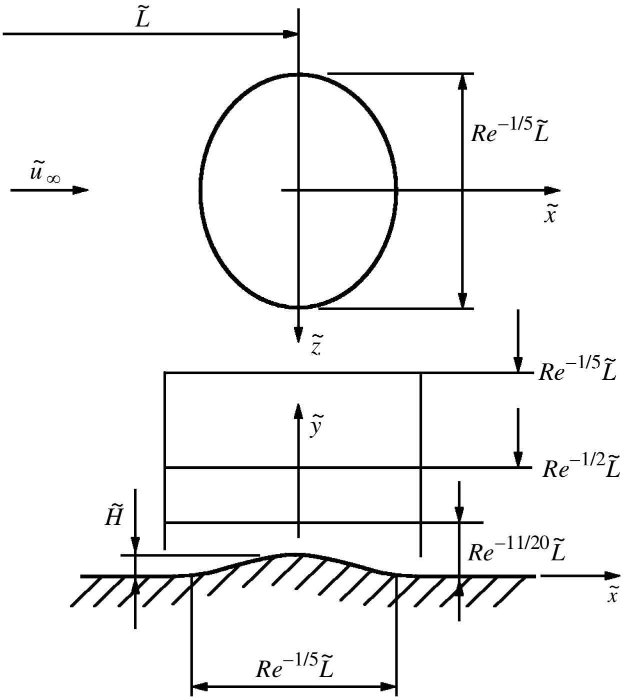

Figure 4. Structure of the local interaction region.

boundary layer to the verge of separation. Rather, the approach to separation occurs much more slowly and is caused primarily by the existence of an adverse pressure gradient acting over a distance of order one on a typical boundary layer length-scale. As a consequence, the effects of surface-mounted obstacles and blowing or suction have received much less attention compared with the case of triple deck theory. Nevertheless, it seems important to study such effects, because they also offer a relatively simple means to determine the response of a two-dimensional marginally separated boundary layer to three-dimensional disturbances. This is one of the aims of the present investigation. In addition, an attempt is made to include dense gas effects which have recently found wide spread interest in the field of gasdynamics into interaction theories which have focused so far primarily on incompressible media or dilute gases.

A different form of three-dimensional effect, not considered here, occurs if the oncoming boundary layer is no longer strictly planar. Flows of this latter type have been investigated by Brown (1985), Duck (1989), Zametaev (1989) and more recently by Kluwick & Reiterer (1998), Reiterer (1998) and F. T. Smith (1998, personal communication).

2. Three-dimensional disturbances of a two-dimensional marginally separated boundary layer

In this section we consider interaction processes which occur if a two-dimensional almost separated boundary layer on a locally flat plate encounters a three-dimensional surface-mounted obstacle. This is sketched in figure 4, where $\tilde{x}, \tilde{y}, \tilde{z}$ and $\tilde{L}$ denote

Cartesian coordinates and a characteristic length, respectively. $\tilde{u}, \tilde{v}$ and $\tilde{w}$ are the corresponding velocity components and the subscript ∞ denotes the reference value of the various flow quantities in the external inviscid flow region.

Following Stewartson *et al.* (1982), we start with the investigation of low Mach number, i.e. incompressible flows. In the large Reynolds number limit,

$$Re = \frac{\tilde{u}_\infty \tilde{L}}{\tilde{\nu}_\infty} \to \infty, \tag{2.1}$$

which is of interest here the extent of the interaction region in the streamwise and lateral direction is of the order $Re^{-1/5}\tilde{L}$ and the interaction region exhibits a three-tiered structure similar to the case of strictly two-dimensional flow (Hackmüller & Kluwick 1990*a*). Viscous effects are of importance in a thin layer (lower deck) adjacent to the wall only. The role of the main deck which comprises most of the boundary layer is to transmit displacement effects exerted by the lower deck to the external flow region (upper deck) where they lead to an inviscid pressure response. Simple order of magnitude estimates indicate that the presence of a surface-mounted obstacle inside the interaction region generates pressure disturbances (non-dimensional with $\tilde{\rho}_\infty \tilde{u}_\infty^2$) of the order $Re^{-1/5}\tilde{H}/\tilde{L}$, where $\tilde{\rho}$ and $\tilde{H}$ characterize the density of the fluid and the height of the obstacle. If the formation of a Goldstein separation singularity is to be avoided, these pressure disturbances must be of the same order of magnitude as the pressure disturbances caused by the interaction process, i.e. of order $Re^{-1/2}$. This immediately yields the estimate

$$H = \frac{\tilde{H}}{\tilde{L}} = O(Re^{-7/10}) \tag{2.2}$$

for the height of obstacles, which is compatible with the assumption of a marginally separated boundary layer.

To investigate the flow properties of the lower deck region, it is convenient to introduce the stretched coordinates:

$$\left.\begin{aligned} x_* &= Re^{1/5}\frac{\tilde{x}-\tilde{L}}{\tilde{L}}, \quad y_* = Re^{11/20}\left[\frac{\tilde{y}}{\tilde{L}} - Re^{-7/10}h_0(x_*, z_*)\right], \\ z_* &= Re^{1/5}\frac{\tilde{z}}{\tilde{L}}. \end{aligned}\right\} \tag{2.3}$$

The expansions for the velocity components and the pressure gradient then assume the form:

$$\left.\begin{aligned} \frac{\tilde{u}}{\tilde{u}_\infty} &= Re^{-1/20}\frac{p_{00}}{2}y_*^2 + Re^{-1/4}A_1(x_*, z_*) + \cdots, \\ \frac{\tilde{v}}{\tilde{u}_\infty} &= Re^{-3/5}\left[\frac{p_{00}}{2}\frac{\partial h_0}{\partial x_*} - \frac{1}{2}\frac{\partial A_1}{\partial x_*}\right] + \cdots, \\ \frac{\tilde{w}}{\tilde{u}_\infty} &= Re^{-2/5}w_2(x_*, y_*, z_*) + \cdots, \\ \frac{\tilde{L}}{\tilde{\rho}_\infty \tilde{u}_\infty^2}\frac{\partial \tilde{p}}{\partial \tilde{x}} &= p_{00} + \cdots + Re^{-3/10}\frac{\partial p_i}{\partial x_*} + \cdots. \end{aligned}\right\} \tag{2.4}$$

Here $h_0(x_*, z_*), p_{00}$ and p_i denote, respectively, the shape of the surface-mounted obstacle, the imposed pressure gradient and the leading-order induced pressure disturbances. It should be noted that, in contrast to the corresponding triple deck problem studied by Smith *et al.* (1977), the induced lateral velocity component is much smaller than the induced velocity disturbances in the streamwise direction.

The function $A_1(x_*, z_*)$ which has the meaning of the axial wall shear stress distribution remains arbitrary if terms of order $Re^{-1/4}$ and $Re^{-3/5}$ in $\tilde{u}/\tilde{u}_\infty$ and $\tilde{v}/\tilde{u}_\infty$ only are taken into account. In order to determine $A_1(x_*, z_*)$ it is necessary to continue these expansions to higher order which is possible if this quantity satisfies a solvability condition of the form derived in Stewartson *et al.* (1982). Matching of the lower deck, main deck and upper deck solutions and introducing suitably transformed quantities A, h, P, W, X, Y, Z in place of $A_1, h_0, p_i, w_2, x_*, y_*, z_*$ finally yields the interaction equations (Hackmüller & Kluwick 1990*a*):

$$\left.\begin{aligned} A^2(X,Z) - X^2 + \Gamma &= -\int_{-\infty}^{X} \frac{1}{\sqrt{X-t}}\left[\frac{\partial P}{\partial t} + \int_{-\infty}^{t} \frac{\partial^2 P}{\partial Z^2}\,\mathrm{d}\tau\right]\mathrm{d}t, \\ P(X,Z) &= \frac{1}{2\pi}\int_{-\infty}^{\infty}\int_{-\infty}^{\infty} \frac{f_{\xi\xi}(\xi,\infty) - f_{\xi\xi}(\xi,\zeta)}{\sqrt{(\xi-X)^2+(\zeta-Z)^2}}\,\mathrm{d}\xi\,\mathrm{d}\zeta + \frac{1}{\pi}\int_{-\infty}^{\infty}\frac{f_\xi(\xi,\infty)}{X-\xi}\,\mathrm{d}\xi, \\ f(X,Z) &= A(X,Z) - h(X,Z), \\ A(X,Z) &\sim |X|, \quad X \to \pm\infty. \end{aligned}\right\} \tag{2.5}$$

The quantity Γ entering these equations characterizes the deviation of the controlling parameter k from its critical value k_0 just as in the case of strictly two-dimensional flow. Once $A(X,Z)$ and $P(X,Z)$ have been determined the leading-order contribution of the cross-flow velocity can be obtained in a separate step by solving the linear problem,

$$\left.\begin{aligned} \tfrac{1}{2}Y^2\frac{\partial W}{\partial X} &= -\frac{\partial P}{\partial Z} + \frac{\partial^2 W}{\partial Z^2}, \\ W &\sim -\frac{2}{Y^2}\int_{-\infty}^{X}\frac{\partial P}{\partial Z}\,\mathrm{d}\xi, \quad Y\to\infty, \end{aligned}\right\} \tag{2.6}$$

which in turn yields the lateral wall shear stress distribution:

$$\frac{\partial W}{\partial Y}(X,0,Z) = \frac{(-\frac{1}{4})!(\frac{1}{2})!}{2^{1/4}\pi}\int_{-\infty}^{X}\frac{\partial P}{\partial Z}\frac{1}{(X-\xi)^{3/4}}\,\mathrm{d}\xi. \tag{2.7}$$

So far the considerations have concentrated on incompressible flows but, using the arguments of Stewartson *et al.* (1982), equations (2.5) and (2.6) can readily be shown to describe also subsonic flows of perfect gases past adiabatic walls if the field quantities and the coordinates are suitably redefined. Moreover, the range of validity of the interaction equations is easily extended to include the supersonic flow regime by a straightforward modification of the pressure–displacement relationship. Finally, following the analysis of Hackmüller & Kluwick (1990*b*) for strictly two-dimensional flow, the interaction equation (2.5) can readily be generalized to account for the effects of blowing and suction. However, flows of these latter types have not yet been investigated.

The solution of equations (2.5), (2.6) requires substantial numerical efforts. Further analytical progress is possible, however, if the shape of the surface-mounted obstacle varies slowly in the lateral direction so that h depends on the slow variable $\bar{Z} = \varepsilon Z$

rather than Z, where ε is a small perturbation parameter. As to be expected, one then finds that the pressure–displacement law reduces to its two-dimensional version formally. As a result the integro-differential equation for A assumes the form,

$$A^2(X,Z) - X^2 + \Gamma = \int_X^\infty \frac{f_{\xi\xi}(\xi,\bar{Z})}{\sqrt{\xi - X}}\,\mathrm{d}\xi, \tag{2.8}$$

which differs from its two-dimensional counterpart only insofar as $\bar{Z}$ enters as a parameter.

Equation (2.8) has been studied intensively in the past (Hackmüller & Kluwick 1989, 1990*a*, *b*). In the following, therefore, we shall assume that the width and length of the obstacle under consideration are of comparable magnitude. As a result, the full three-dimensional form of the interaction equations (2.5) has to be solved numerically. To this end it is convenient to introduce the decompositions,

$$A(X,Z) = A_\infty(X) + \bar{A}(X,Z), \qquad f(X,Z) = f_\infty(X) + \bar{f}(X,Z), \tag{2.9}$$

where $f_\infty(X) = f(X,\infty)$ and $A_\infty(X) = A(X,\infty)$ satisfy equation (2.8). Fourier transformation of the equation for $\bar{A}$ with respect to Z then leads to

$$\begin{aligned} &2A_\infty(X)\bar{A}^*(X,\omega) + (\bar{A}^2(X,Z))^* \\ &\quad= \int_X^\infty \frac{\Delta^*\bar{f}^*(\xi,\omega)}{\sqrt{\xi - X}}\,\mathrm{d}\xi - \int_{-\infty}^\infty \sqrt{\omega}G((\xi - X)\omega)\Delta^*\bar{f}^*(\xi,\omega)\,\mathrm{d}\xi, \\ &\qquad\qquad \bar{A}^*(X,\omega) \to 0, \quad X \to \pm\infty, \end{aligned} \tag{2.10}$$

where

$$\left.\begin{aligned} G((\xi - X)\omega) &= \frac{2\sqrt{\omega}}{\pi}\int_0^\infty \operatorname{sgn}(X - \xi - u^2)\bar{K}_1(|X - \xi - u^2|\omega)\,\mathrm{d}u, \\ \Delta^* = \frac{\partial^2}{\partial\xi^2} - \omega^2, \quad \bar{K}_1(s) &= K_1(s) - \frac{1}{s}, \quad \bar{A}^*(X,\omega) = \int_{-\infty}^\infty \bar{A}(X,Z)\mathrm{e}^{-\mathrm{i}\omega Z}\,\mathrm{d}Z \end{aligned}\right\} \tag{2.11}$$

and K_1 denotes the modified Bessel function of first order (Kluwick *et al.* 1997).

As a specific example we consider surface-mounted obstacles of the form,

$$\left.\begin{aligned} \bar{h}(X,Z) &= \begin{cases} H(1 - X^2)^3\mathrm{e}^{-(Z/B)^2} & \ldots |X| \leqslant 1, \\ 0 & \ldots |X| \geqslant 1, \end{cases} \\ h_\infty(X) &= 0, \end{aligned}\right\} \tag{2.12}$$

which are symmetric with respect to both the X- and Z-axes. The parameters H and B characterize the height of the obstacle and its extent in the lateral direction.

Equations (2.10), (2.11) were cast into finite-difference form using central differences in X and the trapezoidal rule to evaluate the integrals. The resulting set of equations was then solved iteratively by approximating the term $(\bar{A}^2)^*$ with the results obtained from the previous iteration. Starting from a suitable choice for $\bar{A}(X,Z)$ the iterations were carried out until the corrections calculated in one iteration step were less than 10^{-4} in absolute value in all meshpoints.

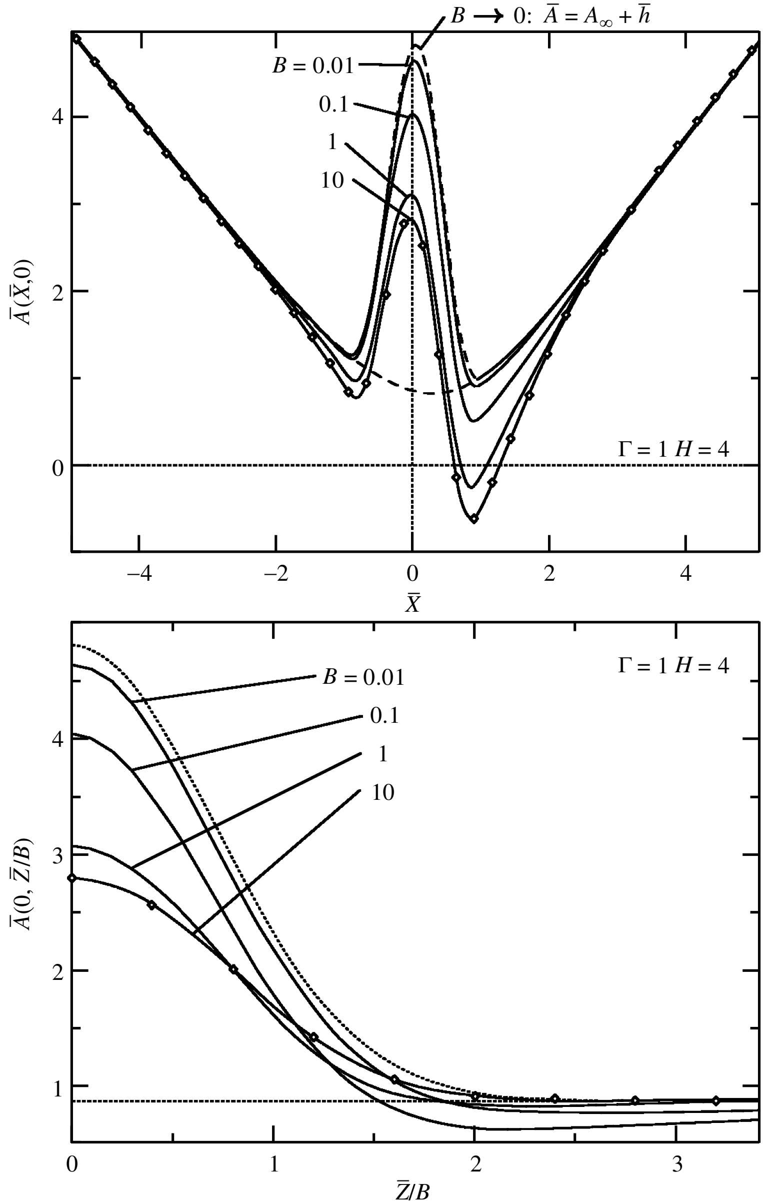

Figure 5. Distribution of the x-component of the wall shear stress for $\Gamma = 1$, $H = 4$ and various values of B (Kluwick *et al.* 1997). $---$, A_∞, $A_\infty + \bar{h}$; $\Diamond$, quasi-two-dimensional flow.

Figure 5 shows typical results for the case that the unperturbed boundary layer is at the verge of separation but still attached as indicated by the wall shear stress distribution $A_\infty(X)$ on a locally flat surface. For large values of B, the numerical solutions of the interaction equations (2.5) are found to be in excellent agreement with the solution of equation (2.8) for quasi-two-dimensional flows obtained by Hackmüller & Kluwick (1990a), which predict the formation of a separation zone on the leeward

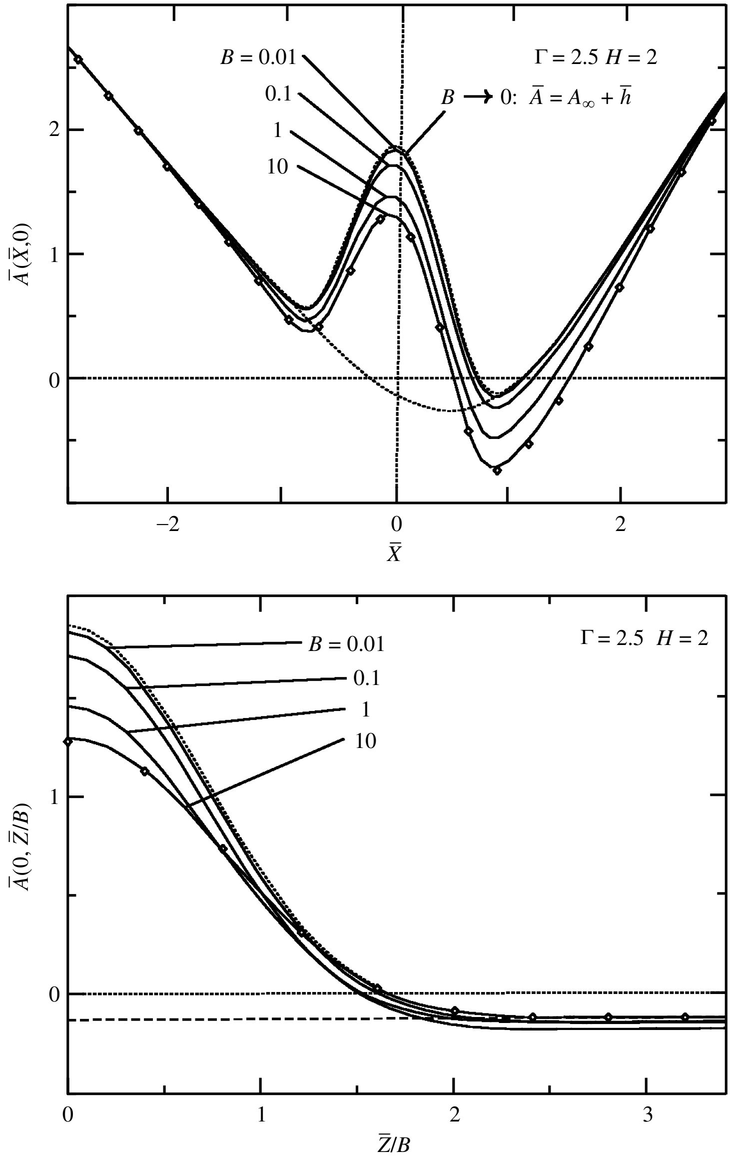

Figure 6. Distribution of the x-component of the wall shear stress for $\Gamma = 2.5$, $H = 2$ and various values of B (Kluwick *et al.* 1997). — — —, A_∞, $A_\infty + \bar{h}$; $\Diamond$, quasi-two-dimensional flow.

side of the protrusion. As the lateral extent B of the protrusion decreases, the axial component A of the wall shear stress is seen to increase. As a consequence, the separated flow region shrinks and eventually vanishes. Finally, inspection of the results for $B \ll 1$ and the curve $A_\infty(X)$ shows that slender protrusions lead to an increase of the wall shear stress almost everywhere. Indeed, analytical considerations indicate that $A(X, Z)$ approaches the limiting form,

$$A(X, Z) \sim A_\infty(X) + h(X, Z) \quad \text{as} \quad B \to 0 \tag{2.13}$$

PHILOSOPHICAL TRANSACTIONS OF THE ROYAL SOCIETY A MATHEMATICAL, PHYSICAL & ENGINEERING SCIENCES

(Reiterer 1998). Comparison with the numerical solution for the smallest value of $B = 0.01$ included in figure 5 yields reasonably good agreement.

Representative results when the unperturbed boundary layer is no longer attached but is marginally separated are displayed in figure 6. The distributions of the axial wall shear stresses follow the same general trends as in the attached flow case, i.e. $A(X, Z)$ assumes its lowest values on protrusions with large lateral extent B where the results are in excellent agreement with the predictions following from the theory for quasi-two-dimensional flow. With decreasing width B of the protrusion the axial wall shear stresses are again found to increase and the distributions eventually asymptote the limiting form (2.13) as B tends to zero.

3. Sweep effects

Following the discussion of three-dimensional disturbances imposed on a two-dimensional marginally separated boundary layer, let us have a brief look at sweep effects. As before we concentrate on disturbances caused by surface-mounted obstacles placed into a boundary layer which does not vary in the spanwise direction. In contrast to the type of flow considered so far, however, we now allow for a non-zero cross-flow velocity $\tilde{w}_\infty$ in the external inviscid flow region.

Asymptotic analysis of the flow then closely follows the steps outlined earlier which thus will not be repeated here. It suffices to note that the cross-flow velocity component (non-dimensional with $\tilde{u}_\infty$) in the viscous wall region of the unperturbed boundary layer is a linear function of the scaled wall distance:

$$w \sim Re^{-1/20} b_{00} y_* + \cdots + Re^{-1/5} w_1(x_*, y_*, z). \tag{3.1}$$

Here b_{00} is an arbitrary constant which cannot be determined from a local analysis. The magnitude of the induced cross-flow velocities is a direct consequence of the magnitude of the normal velocity components and the assumed extent of $O(\tilde{L})$ of the surface-mounted obstacle in the spanwise direction. One then finally obtains the integro-differential equation for the x-component A of the wall shear in the form,

$$A^2(X, Z) - X^2 + \Gamma + 2\int_{-\infty}^{X} A_Z(\xi, Z)\,\mathrm{d}\xi = \int_X^\infty \frac{A_{\xi\xi}(\xi, Z) - h_{\xi\xi}(\xi, Z)}{\sqrt{\xi - X}}\,\mathrm{d}\xi, \tag{3.2}$$

where, as usual, all quantities are suitably scaled to remove the various parameters which enter the description of the boundary layer upstream of the local interaction zone. As in the preceding section Γ and h characterize, respectively, the deviation of the controlling parameter from its critical value and the shape of the surface-mounted obstacle.

If the controlling parameter is sufficiently smaller than its critical value, i.e. in the limit $\Gamma \to -\infty$, viscous–inviscid interaction accounted for by the term on the right-hand side of equation (3.2) is of little importance and can be neglected in a first approximation. The governing equation for A then differs from its strictly two-dimensional, non-interacting counterpart by the integral $\int_{-\infty}^{X} A_Z(\xi, Z)\,\mathrm{d}\xi$ only. Differentiation with respect to X then leads to the first order partial differential equation,

$$A_Z + AA_X = X, \qquad \Gamma \to -\infty. \tag{3.3}$$

Following common practice in the theory of partial differential equations, it appears appropriate to denote the characteristics $\zeta =$ const. of this limiting equation

$$\left.\frac{\mathrm{d}X}{\mathrm{d}Z}\right|_{\zeta=\mathrm{const.}} = A(X,Z), \tag{3.4}$$

which can be shown to represent wall-streamlines, as subcharacteristics of the full interactive equation (3.1). This ties in nicely with earlier analysis by Wang (1971), who argued that the streamlines inside a classical boundary layer with imposed pressure gradient should be interpreted as subcharacteristics of the Navier–Stokes equations. If the dependence of the field quantities from the distance normal to the wall is specified in advance by specific functions, as for example when one uses integral methods, these subcharacteristics become characteristics of the reduced set of equations. However, in the theory of marginally separated flows the variation of the field quantities in the viscous sublayer with the distance normal to the wall is known also in advance (in leading order) as pointed out earlier and the same for all possible solutions. In a sense, therefore, this theory can be viewed as an asymptotically correct version of an integral method. Furthermore, since the viscous sublayer is so thin, the streamlines there almost collapse onto the wallstreamlines and, as a consequence, the evolution equation (3.3) for the 'shape function' $A(X,Z)$ contains a single characteristic only.

Using the definition (3.4) of subcharacteristics the full interaction equation (3.2) can be cast into the form,

$$\left.\frac{\mathrm{d}A}{\mathrm{d}Z}\right|_{\zeta} = \frac{1}{2}\int_X^{\infty} \frac{A_{\xi\xi\xi}(\xi,Z) - h_{\xi\xi\xi}(\xi,Z)}{\sqrt{\xi - Z}}\,\mathrm{d}\xi + X. \tag{3.5}$$

According to this relationship, the derivative of A on $\zeta =$ const. in a point P of the X,Z-plane is fully determined by the integral on the right-hand side, which extends from X_P to ∞. As a consequence, the region of dependence of P coincides with the shaded region above the curve $\zeta =$ const. through P as sketched in figure 7. This immediately suggests one possibility to solve equation (3.2) numerically if the surface-mounted obstacle is bounded in the Z-direction so that $h(X,Z) \equiv 0$ for $Z < Z_{\min}$, say. In this unperturbed region A is independent of Z and the solution agrees with the result for strictly two-dimensional flows past a flat wall, which then serves as the initial condition for the integration along subcharacteristics into the Z-domain where $h(X,Z)$ is non-zero. Actually, however, it was found easier to solve the interaction equation in its original form (3.2) using backward differences to approximate the derivatives of $A(X,Z)$ with respect to Z and treating the interaction term in exactly the same way as in the case of two-dimensional flows.

It is useful to consider first surface-mounted obstacles whose height varies only slowly in the spanwise direction. The integral term on the left-hand side of equation (3.2) then is small and can be neglected in a first approximation. Consequently, the governing equation for $A(X,Z)$ reduces to the relationship,

$$A^2(X,Z) - X^2 + \Gamma = \int_X^{\infty} \frac{A_{\xi\xi}(\xi,Z) - h_{\xi\xi}(\xi,Z)}{\sqrt{\xi - X}}\,\mathrm{d}\xi, \tag{3.6}$$

which differs from the interaction equation for strictly two-dimensional flows derived by Hackmüller & Kluwick (1989) only insofar as Z enters as a parameter. As a result,

PHILOSOPHICAL TRANSACTIONS OF THE ROYAL SOCIETY A MATHEMATICAL, PHYSICAL & ENGINEERING SCIENCES

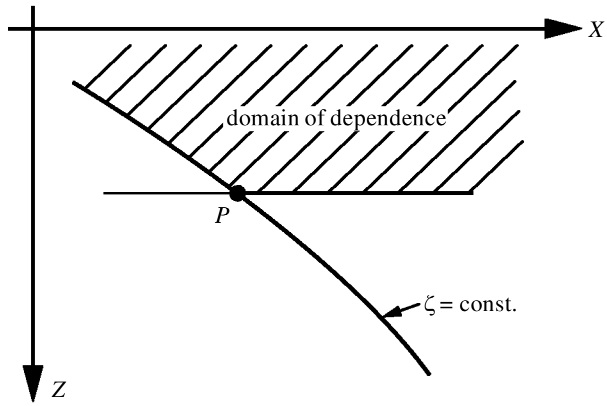

Figure 7. Domain of dependence of point P in the X, Z-plane. —, subcharacteristic

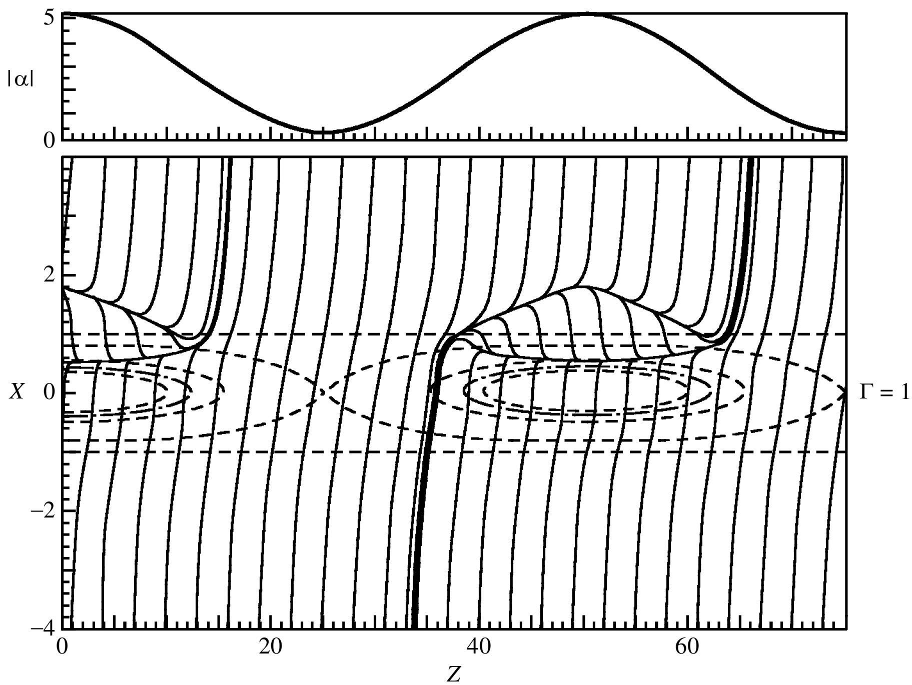

Figure 8. Wallstreamline pattern generated by a periodic array of surface-mounted obstacles on a swept wing (Hackmüller & Kluwick 1991). – – –, contour lines; —, wallstreamlines.

it is possible to calculate the X-component of the wall shear stress component in different planes Z = const. independently. If desired, these results can be used in a subsequent step to determine global flow properties as for example the shape of subcharacteristics, i.e. wallstreamlines.

As a specific case we consider protrusions of the shape,

$$\left.\begin{aligned} h(X,Z) &= \alpha(Z)(X^2-1)^3, \\ \alpha(Z) &= \alpha_a \cos(2\pi Z/\mu) + \alpha_b, \end{aligned}\right\} \tag{3.7}$$

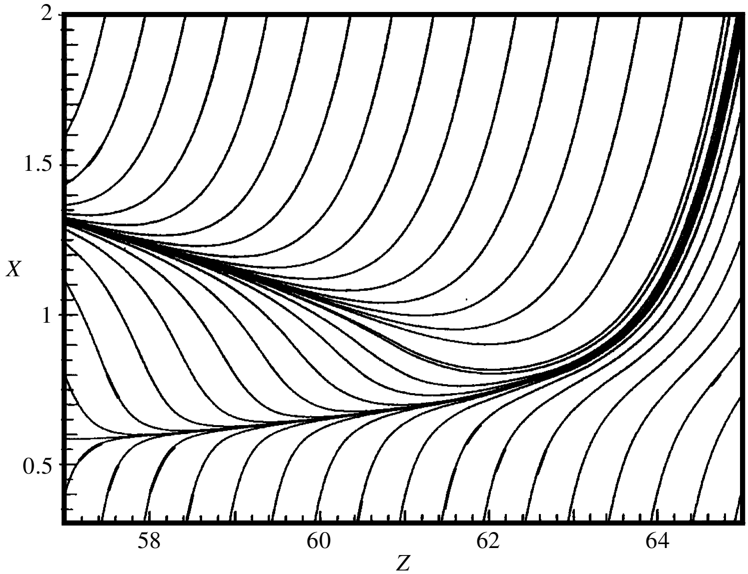

Figure 9. Detail of wallstreamline pattern displayed in figure 8.

whose height varies periodically in the spanwise direction. Here α_a and α_b are arbitrary constants which determine the maximum and minimum height of the protrusion while the parameter $\mu \ll 1$ characterizes the slow variation of the geometry with the coordinate Z. In planes $Z =$ const. the shape of the protrusion agrees with the form of the two-dimensional obstacles studied by Hackmüller & Kluwick (1989), and their results, therefore, represent local solutions of equation (3.6) for the type of flow considered here. The wallstreamline pattern constructed from these results is shown in figure 8, where the dashed lines represent contour lines $h(X, Z) =$ const. In addition, the dot-dash line indicates the minimum height of the protrusion which is necessary to cause separation again as predicted by the results of Hackmüller & Kluwick (1989). As seen from figure 8, the protrusion exceeds this 'critical' height for limited ranges of Z only which repeat themselves periodically. In these regimes small open separation bubbles form, downstream of the protrusion, which experience a mass flux from the left to the right. It is interesting to note that no curves that have the meaning of separation or reattachment lines can be identified in the wallstreamline pattern. This can be seen more clearly from figure 9, which is a blow-up of the open end of one of the separation bubbles. Owing to the displacement of the fluid in the direction normal to the wall there exist regions of high density of wallstreamlines which, however, do not form envelopes.

A solution of the fully three-dimensional form (3.2) of the interaction equation is shown in figure 10, where we consider disturbances caused by an isolated hump,

$$h(X, Z) = 4(\cos^2 Z)(1 - X^2)^3, \qquad -1 \leqslant X \leqslant 1, \quad -\pi/2 \leqslant Z \leqslant \pi/2. \tag{3.8}$$

The calculations were initiated at $Z = -1.65$, where $A(X, Z)$ is known from the theory of strictly two-dimensional flows on a locally flat wall, and were then advanced in the positive Z-direction. As before the height of the obstacle is large enough to cause separation, as can be seen from the wall shear distribution at $Z = -0.6$, where

PHILOSOPHICAL TRANSACTIONS OF THE ROYAL SOCIETY A MATHEMATICAL, PHYSICAL & ENGINEERING SCIENCES

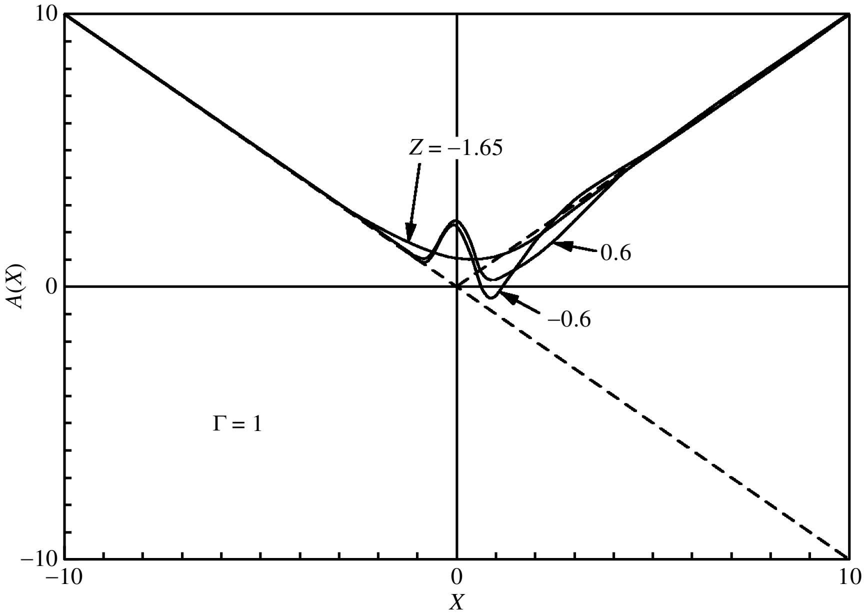

Figure 10. Distribution of the x-component of the wall shear stress for $\Gamma = 1$ (Hackmüller 1991).

the results are found to be in good agreement with the predictions of equation (3.6) holding for quasi-two-dimensional flows. With increasing Z, however, the error of this approximation increases rapidly. This is evident from the results at $Z = 0.6$ which, according to this approximation, should coincide with those at $Z = -0.6$. In reality, however, the boundary layer at $Z = 0.6$ is attached rather than separated owing to the three-dimensional relief of the flow not accounted for in the quasi-two-dimensional approximation.

4. Dense gas effects

So far the considerations have focused on flows of incompressible media or dilute gases which can be treated as perfect gases. In the last 15 years, however, the flow properties of dense gases, i.e. gases in the general neighbourhood of the thermodynamic critical point, have received increasing interest. Studies in which thermoviscous effects were neglected have shown that such flows may lead to a number of new and unexpected phenomena provided that the molecular complexity of the medium under consideration is sufficiently high (see, for example, Kluwick 1991). These effects can be inferred from the properties of a single thermodynamic quantity, the so-called fundamental derivative,

$$\Gamma = \frac{\tilde{v}^3}{2\tilde{c}^2}\left(\frac{\partial^2 \tilde{p}}{\partial \tilde{v}^2}\right)_{\tilde{s}}. \tag{4.1}$$

Here $\tilde{c}$, $\tilde{p}$, $\tilde{v} = 1/\tilde{\rho}$ and $\tilde{s}$ denote, respectively, the speed of sound, the pressure, the specific volume and the entropy. According to equation (4.1), Γ characterizes the curvature of isentropes in the $\tilde{p}, \tilde{v}$-diagram. In the case of dilute gases $\Gamma = (\gamma + 1)/2$, where γ is the ratio of the specific heats and thus has a lower limit equal to one corresponding to media of high molecular complexity, i.e. media formed by molecules with a large number of internal degrees of freedom. As suggested first by Bethe (1942) and independently by Zel'dovich (1946), this is not true in the dense gas regime, where Γ can assume values less than one or even negative values. Specific examples of negative Γ fluids were provided by Thompson and co-workers (Thompson & Lambrakis 1973; see also Thompson 1991) and include hydrocarbons and fluorocarbons, which are frequently used in engineering applications as, for example, in organic Rankine cycles. In recognition of the pioneering work by Bethe, Zel'dovich and Thompson, they are now commonly referred to as BZT fluids.

If one considers supersonic flows with weak shocks, it can be shown (Bethe 1942) that the resulting entropy and density jumps satisfy the relationship,

$$[\tilde{s}] = \frac{\Gamma_b \tilde{c}_b^2}{6\tilde{T}_b \tilde{\rho}_b^3}[\tilde{\rho}]^3 + \cdots, \tag{4.2}$$

to leading order where the subscript b refers to the upstream state and $\tilde{T}$ denotes the temperature. If $\Gamma_b > 0$, as in the case of dilute gases, the second law of thermodynamics which requires a positive entropy jump is satisfied only if the density jump is positive also. As a consequence, only compression shocks are possible. In contrast, if $\Gamma_b < 0$, only expansion shocks causing a sudden decrease of the density $[\tilde{\rho}] < 0$ are compatible with the second law. This settles a long-standing question concerning the possible existence of expansion shocks; they may form in the dense gas regime of sufficiently complex vapours.

The fact that Γ can assume negative values has yet another interesting consequence, which will be of importance later. To this end we consider the Mach number variation during isentropic expansion. Differentiation of the local Mach number M with respect to $\tilde{v}$ at constant $\tilde{s}$ yields the expression,

$$\frac{1}{M}\frac{\mathrm{d}M}{\mathrm{d}\tilde{v}}\bigg|_{\tilde{s}} = \frac{1}{\tilde{v}}\left[\frac{1}{M^2} + \Gamma - 1\right]. \tag{4.3}$$

Therefore, if stagnation conditions are chosen such that $\Gamma \geqslant 1$ during the subsequent expansion, M increases monotonically with $\tilde{v}$ just as in the case of a perfect gas. However, if the isentrope exhibits a portion where $0 \leqslant \Gamma < 1$ or $\Gamma < 1$, the initial Mach number increase may be followed by a Mach number decrease before M rises again for sufficiently large values of $\tilde{v}$. We, therefore, conclude that the $M, \tilde{v}$-relationship of a BZT fluid may be non-monotonous (Cramer 1991; Kluwick 1993).

Guided by experience with perfect gases, one expects that the shape of the shock polar in the $\tilde{p}, \tilde{v}$-diagram is qualitatively similar to the shape of isentropes, and this turns out to be perfectly true. One thus finds that the shock polar is not a strictly convex curve as in the case of perfect gases but exhibits regions of positive and negative curvature. This in turn leads to rather unconventional properties of steady supersonic flows. For example, compression shocks/expansion wave fans will be generated in flows past compression/expansion ramps if $\Gamma > 0$. If, however, $\Gamma < 0$ in the flow regime under consideration, compression wave fans/expansion shocks will form instead (figure 11).

Following this brief interlude on dense gasdynamics let us return to laminar boundary layers. If the Reynolds number is scaled out as usual, the relevant non-dimensional

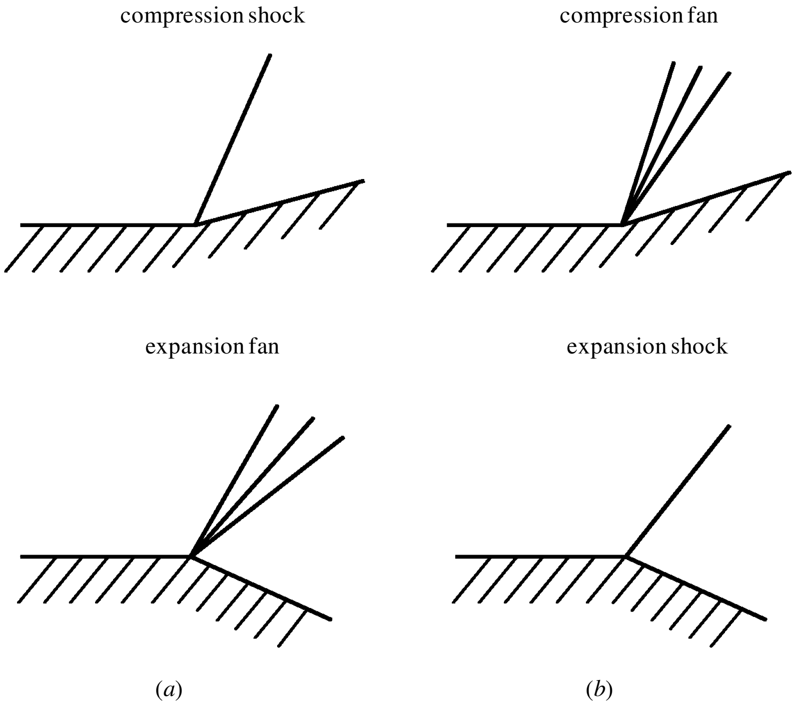

Figure 11. Supersonic flow past a compression/expansion ramp: (a) perfect gas and positive Γ fluids, (b) negative Γ fluids.

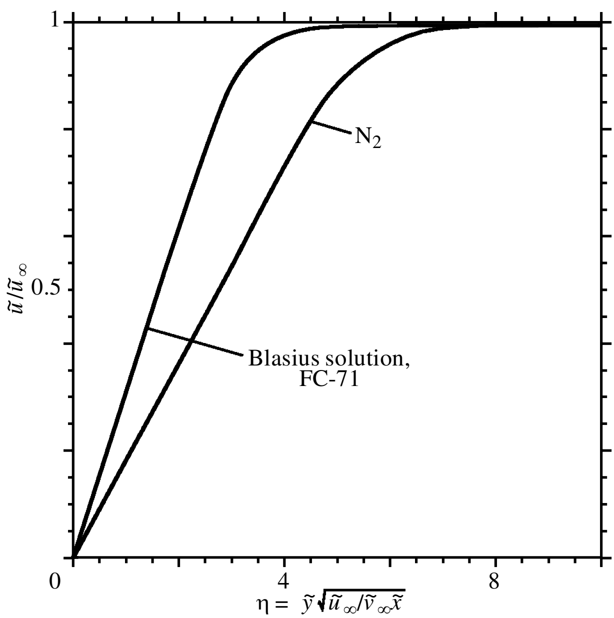

Figure 12. Flat plate boundary layer: $M_\infty = 2$ (Kluwick & Zieher 2000).

PHILOSOPHICAL TRANSACTIONS OF THE ROYAL SOCIETY A MATHEMATICAL, PHYSICAL & ENGINEERING SCIENCES

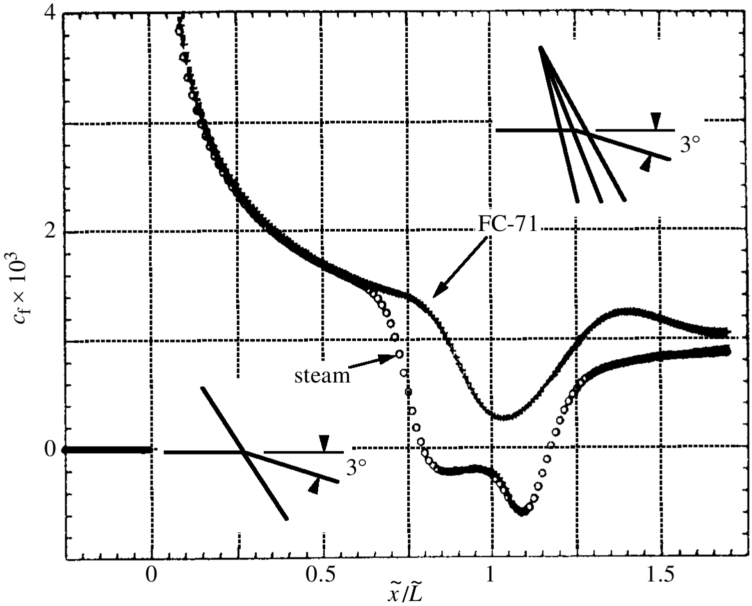

Figure 13. Wall shear stress distribution of a supersonic boundary layer which interacts with a weak compression wave (Park 1994). $M_\infty = 2$, $\tilde{T}_\infty = 646.2$ K, $\tilde{p}_\infty = 8.55$ atm.

groups are the Prandtl number, the thermal expansion coefficient $\tilde{\beta}$ non-dimensional with $\tilde{T}$ and the Eckert number:

$$Pr = \frac{\tilde{\mu}_r \tilde{c}_{pr}}{\tilde{\lambda}_r}, \quad \tilde{\beta}_r \tilde{T}_r, \quad Ec = \frac{\tilde{u}_r^2}{\tilde{c}_{pr} \tilde{T}_r}. \tag{4.4}$$

Here $\tilde{\mu}$, $\tilde{\lambda}$ and $\tilde{c}_p$ denote the dynamic viscosity, the thermal conductivity and the isobaric heat capacity. The subscript 'r' refers to a suitable reference state. Similar to perfect gases the Prandtl number and $\tilde{\beta}_r \tilde{T}_r$ of dense gases are of order one if the immediate vicinity of the thermodynamic critical point is excluded from the considerations. In contrast, however, the Eckert number is no longer of order M_r^2 but of the order $M_r^2/c_{v\infty}$, where $c_{v\infty}$ is the isochoric ideal gas heat capacity evaluated at the critical point temperature non-dimensional with the universal gas constant (Kluwick 1994). $c_{v\infty}$ increases with increasing molecular complexity and typical values for vapours of BZT fluids in the dense gas regime are in the range 100–150 (Cramer 1991). As a consequence, dissipation caused by internal friction can be neglected even at moderately large supersonic Mach numbers. For flows past adiabatic walls, this means that the temperature, and thus also the density, is almost constant across the boundary layer. As an example, figure 12 shows the velocity distributions in a flat plate boundary layer with zero pressure gradient and $M_\infty = 2$ for nitrogen (N_2) and the BZT fluid FC-71 ($C_{18}F_{39}N$). In the case of nitrogen, dissipative effects cause the velocity profiles to deviate substantially from the Blasius result for incompressible flows, while the solution for FC-71 is indistinguishable from it within graphical accuracy.

Deviations from the classical boundary-layer behaviour are caused not only by the smallness of the Eckert number but also by the unconventional gasdynamic properties

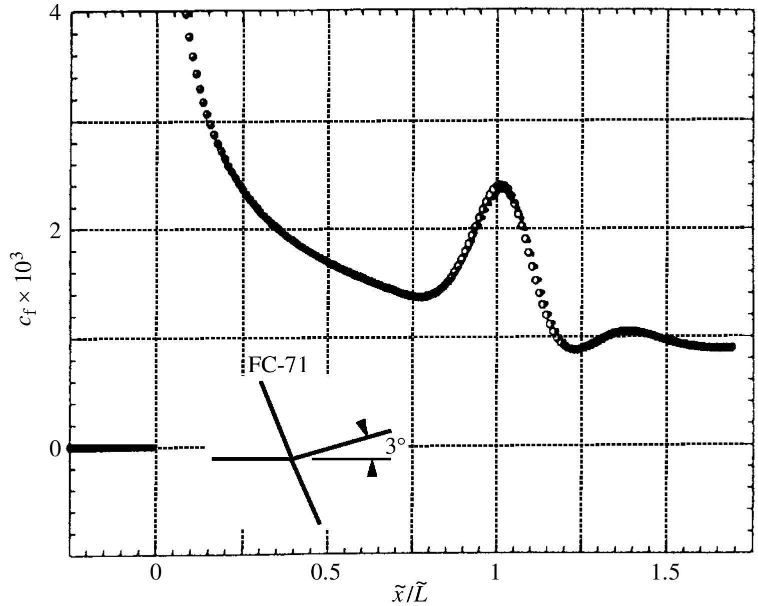

Figure 14. Wall shear stress distribution of a supersonic dense gas boundary layer which interacts with a weak rarefaction shock wave. $M_\infty = 2$, $\tilde{T}_\infty = 646.2$ K, $\tilde{p}_\infty = 8.55$ atm.

of BZT fluids in the external inviscid flow region. As an example, let us consider the interaction of a laminar dense gas boundary layer on a flat plate with a weak oblique shock. Figure 13 shows distributions of the skin friction coefficient calculated numerically by Park (1994) using the full Navier–Stokes equations. In the case of steam the imposed deflection angle of 3° leads to the formation of a compression shock which is strong enough to separate the boundary layer. In contrast, in the case of the BZT fluid FC-71 the deflection of the flow in the external inviscid region does not cause the formation of a shock but it is accomplished by a continuous compression wave fan. Consequently, the pressure disturbances carried by the incoming wave are smoothed out over some distance and the boundary layer remains attached. Finally, if the deflection angle is negative (figure 14), no shock discontinuity can form in a regular fluid such as steam but an expansion shock forms in the BZT fluid FC-71. Across this shock the fluid accelerates, which in turn causes the wall shear to increase rather than to decrease.

In the case of dilute gases the large-Reynolds-number limit of weak shock boundary layer interactions is covered by triple deck theory. According to this theory (see, for example, Smith 1982; Kluwick 1987), only a small portion of the boundary layer (the lower deck adjacent to the wall), where the flow is almost incompressible, takes part actively in the interaction process, while the rest of the boundary layer (the main deck), where compressibility may be important, plays a completely passive role. Furthermore, outside the boundary layer—in the upper deck—we have a weakly perturbed parallel flow where nonlinear effects can be neglected to leading order, which, therefore, is described by the classical theories of Prandtl–Glauert and Ackeret. All this suggests that the basic structure of the interaction process also remains intact in the gas dense gas limit and this can be confirmed for both triple deck theory

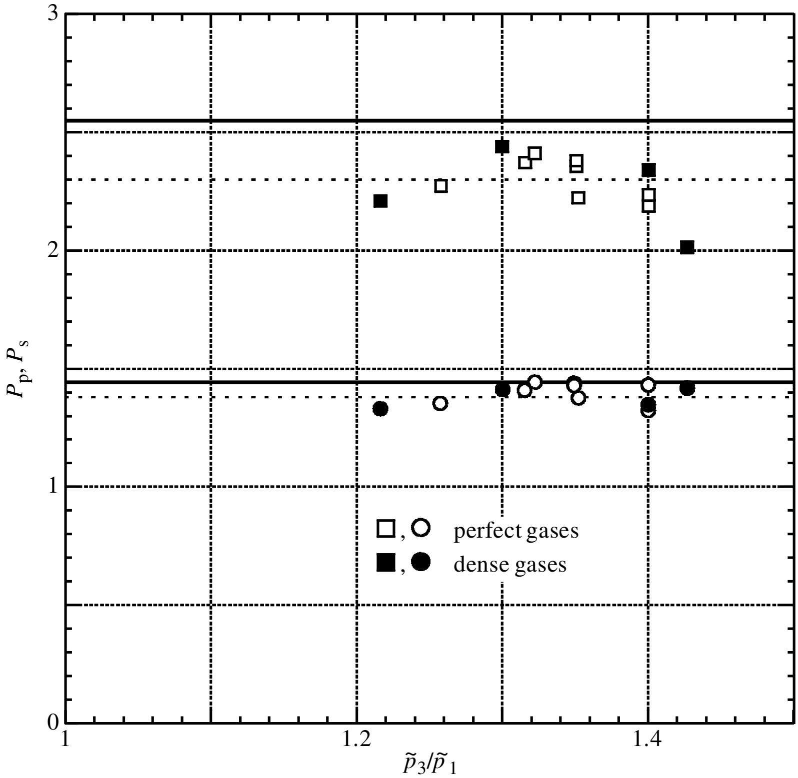

Figure 15. Separation pressure P_s and plateau pressure P_p versus the pressure ratio $\tilde{p}_3/\tilde{p}_1$ for various perfect and dense gases (Park 1994). —, triple deck theory.

(Kluwick 1994), and the theory of marginally separated flows where Stewartsons *et al.*'s (1982) arguments still apply. In the first case one recovers the classical lower deck equations, i.e. the incompressible version of the boundary layer equations with appropriate boundary and matching conditions in parameter-free form if the usual definitions of the transformed quantities are suitably extended (Kluwick 1994). It is interesting to note that the result for the transformed pressure disturbances P,

$$P = \frac{(M_\infty^2 - 1)^{1/4}}{c_{f\infty}^{1/2}} \frac{\tilde{p} - \tilde{p}_\infty}{\tilde{\rho}_\infty \tilde{u}_\infty^2}, \tag{4.5}$$

agrees with the scaling law already proposed in the pioneering study of shock boundary interactions by Chapman *et al.* (1958).

A comparison between numerical results based on the Navier–Stokes equations and the Martin–Hou equation of state, which is able to capture dense gas effects, is shown in figure 15. Here P_s and P_p denote the values of P at separation and the plateau pressure inside the separation bubble. The open and solid symbols denote cases which may be regarded as perfect gases or dense gases, respectively. Furthermore, $\tilde{p}_3/\tilde{p}_1$ is the pressure ratio across the reflection. As predicted by theory, P_s and P_p are basically independent of the pressure ratio and there is no systematic difference between the results for perfect and dense gases. Comparison with the theoretical values $P_s = 1.45$, $P_p = 2.55$ determined by Stewartson & Williams (1969) shows

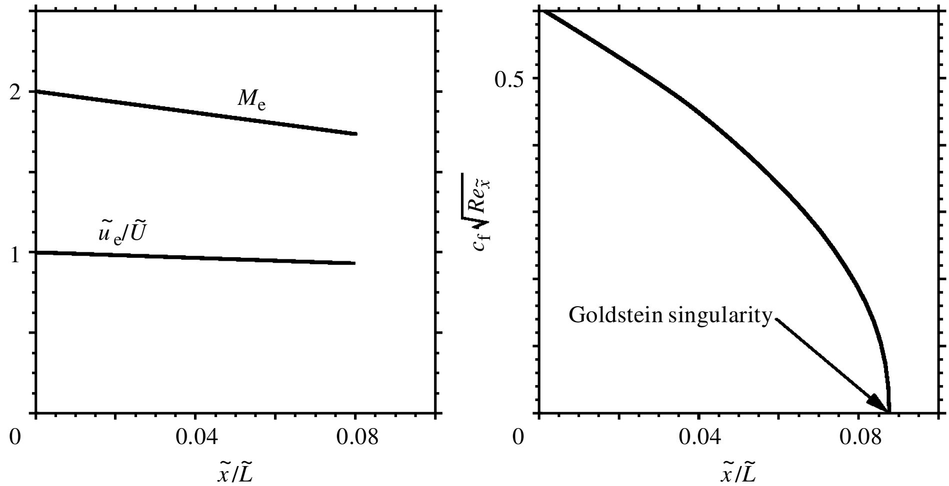

Figure 16. Boundary layer in a linearly retarded flow of N_2: $M_\infty = 2$, $\tilde{\rho}_\infty = 0.2\tilde{\rho}_c$, $\tilde{T}_\infty = 1.001\tilde{T}_c$ (Kluwick & Zieher 2001).

reasonable agreement as far as the separation pressure is concerned but yields larger deviations for the plateau pressure. These discrepancies seem to be caused in part by the fact that the weak shocks investigated in the Navier–Stokes calculations do not generate recirculation zones large enough to exhibit a fully developed plateau region, as indicated also by the scatter of the data.

Following this brief discussion of dense gas local interactions which are triggered by rapid pressure changes, let us return to our main theme, the effect of an adverse pressure gradient acting over a distance of order one on the typical boundary-layer length-scale. As a representative case we consider linearly retarded flows past a thin flat plate. The streamwise velocity component in the external inviscid flow region is then written in the form,

$$\tilde{u}_e = \tilde{U}\left(1 - \frac{\tilde{x}}{\tilde{L}}\right), \tag{4.6}$$

where $\tilde{U}$, $\tilde{x}$ and $\tilde{L}$ denote the freestream velocity at the tip of the plate, the distance measured from the tip of the plate and the length of the plate. As pointed out earlier, the incompressible version of this problem was first investigated by Howarth (1938) and Hartree (1939), who observed that the pressure increase associated with the velocity decrease always leads to eventual separation and that the numerical solution of the boundary-layer equations cannot be extended beyond the separation point. A related result holds for compressible flows with no heat transfer to or from the wall if the medium is a dilute gas (Stewartson 1962), or even for a dense gas provided that the molecular complexity is sufficiently low. As an example of the latter case, we consider nitrogen with freestream conditions $\tilde{\rho}_\infty = 0.2\tilde{\rho}_c$, $\tilde{T}_\infty = 1.001\tilde{T}_c$, $\tilde{M}_\infty = 2$, where $\tilde{\rho}_c$ and $\tilde{T}_c$ denote the critical point density and temperature (figure 16). Decreasing values of $\tilde{u}_e$ lead to decreasing values of the local Mach number M_e at the boundary layer edge. The associated pressure increase causes the local friction coefficient to decrease also and the skin friction distribution eventually tends to zero in an irregular manner.

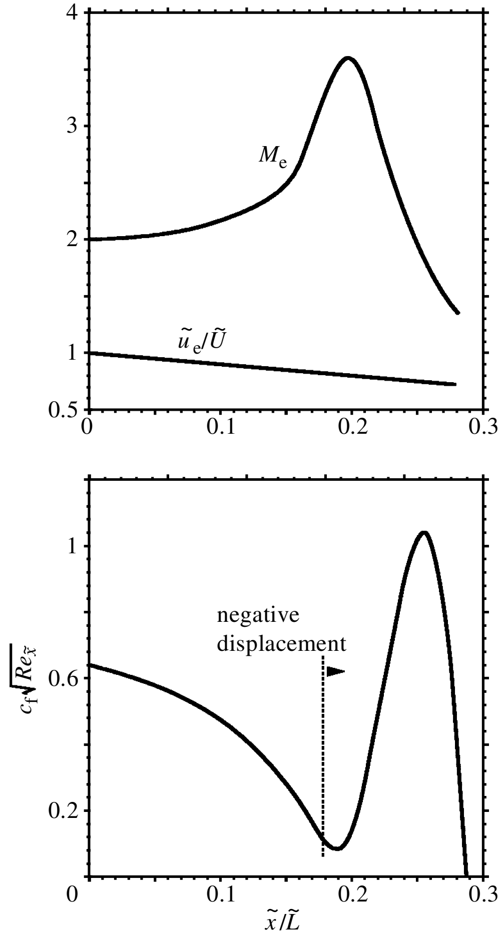

Figure 17. Boundary layer in a linearly retarded flow of the BZT fluid FC-71: $M_\infty = 2$, $\tilde{\rho}_\infty = 0.2\tilde{\rho}_c$, $\tilde{T}_\infty = 1.001\tilde{T}_c$ (Kluwick & Zieher 2000).

Figure 17 shows what happens if the regular fluid nitrogen is replaced by the BZT fluid FC-71. As before, c_f drops initially, but this tendency then comes to a halt and the local friction coefficient starts to increase despite the fact that the pressure gradient is still unfavourable. This leads to the formation of a pronounced local maximum of the wall shear before c_f decreases again and finally vanishes. A more detailed analysis of the flow suggests that this unconventional feature is closely related to the Mach number distribution at the boundary-layer edge. In contrast to the results for nitrogen displayed in figure 16, the isentropic compression of FC-71 initially causes the Mach number in the external inviscid flow region to increase rather than to decrease. Evaluation of the continuity equation outside the boundary layer yields the well-known relationship,

$$\frac{\partial \tilde{v}}{\partial \tilde{y}} = (M_e^2 - 1)\frac{d\tilde{u}_e}{d\tilde{x}}, \tag{4.7}$$

which shows that the normal velocity component $\tilde{v}$ in a decelerating supersonic flow decreases with increasing wall distance $\tilde{y}$. Owing to the fact that the density changes

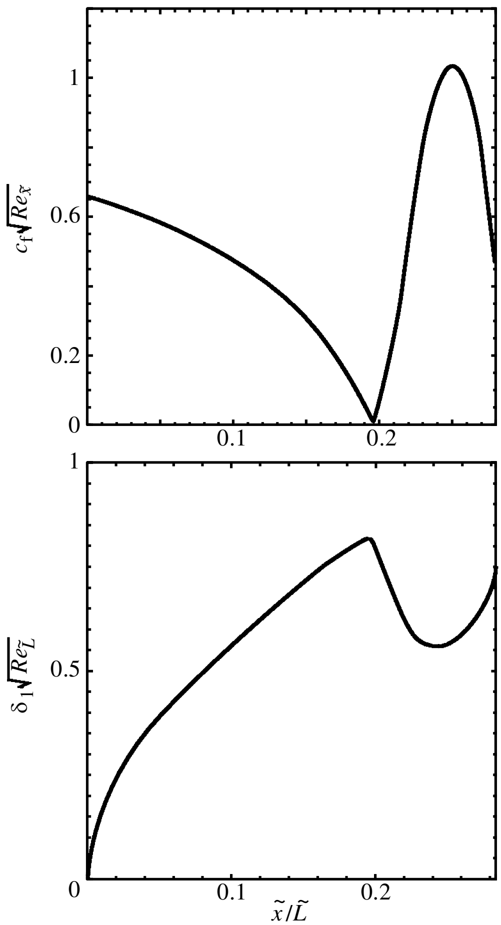

Figure 18. Marginal separation of a supersonic dense gas boundary layer caused by the non-monotonic Mach number variation in the external flow region.

across the boundary layer are small, this is true also for the supersonic outer part of the boundary layer. For sufficiently large values of M_e, one therefore expects that the displacement body felt by the external inviscid flow may shrink rather than expand in the flow direction. This is confirmed by the numerical calculations of Kluwick & Zieher (2001), as indicated in figure 17. The associated momentum influx into the boundary layer then is able to overcome the onset of separation and causes the wall shear stress to rise sharply. Eventually, however, the Mach number starts to drop, which in turn quenches this effect. As a consequence, the local skin friction coefficient also drops and the formation of a separation singularity is inevitable. Nevertheless, the results plotted in figure 17 clearly show that dense gas effects may be used to delay separations.

Furthermore, if the freestream Mach number is slightly reduced while the stagnation conditions are kept fixed, the minimum in the wall shear stress distribution is found to decrease and one finally obtains the limiting case shown in figure 18. The wall shear vanishes in a single point but immediately recovers. At the point of zero wall shear, the displacement body exhibits a sharp corner. Of course, this is a case of marginal separation and work in progress strongly suggests that the associated local interaction process is of classical form. It is triggered, however, by a non-classical mechanism, the non-monotonous Mach number variation during isentropic compression of a dense gas.

References

Bethe, H. A. 1942 The theory of shock waves for an arbitrary equation of state. Report no. 575, Office of Scientific Research and Development, Washington.

Brown, S. N. 1985 Marginal separation of a three-dimensional boundary layer on a line of symmetry. *J. Fluid Mech.* **158**, 95–111.

Chapman, D. R., Kuehn, D. M. & Larson, H. K. 1958 Investigation of separated flows in supersonic and subsonic streams with emphasis on the effect of transition. NACA report no. 1356.

Cramer, M. S. 1991 Nonclassical dynamics of classical gases. In *Nonlinear waves in real fluids* (ed. A. Kluwick), pp. 91–145.

Duck, P. W. 1989 Three-dimensional marginal separation. *J. Fluid Mech.* **202**, 559–575.

Goldstein, S. 1948 On laminar boundary-layer flow near a position of separation. *Q. J. Mech. Appl. Math.* **1**, 43–69.

Hackmüller, G. 1991 Zwei- und dreidimensionale marginale Ablösung von Strömungsgrenzschichten. PhD thesis, Vienna University of Technology.

Hackmüller, G. & Kluwick, A. 1989 The effect of a surface mounted obstacle on marginal separation. *Z. Flugwiss. Weltraumforsch.* **13**, 365–370.

Hackmüller, G. & Kluwick, A. 1990*a* Effects of 3-D surface mounted obstacles on marginal separation, In *Separated Flows and Jets, IUTAM Symp., Novosibirsk, USSR* (ed. V. V. Kozlov & A. V. Dovgal), pp. 55–65. Springer.

Hackmüller, G. & Kluwick, A. 1990*b* Effects of surface geometry and suction/blowing on marginal separation. In *Proc. 3rd Int. Congress of Fluid Mechanics, Cairo, Egypt, 2–4 January 1990*, vol. II, pp. 725–732.

Hartree, D. R. 1939 A solution of the laminar boundary-layer equations for retarded flow. Memor. Aero. Res. Coun., London, no. 2426 (spec. vol. I).

Howarth, L. 1938 On the solution of the laminar boundary layer equations. *Proc. R. Soc. Lond.* A **164**, 547–579.

Kluwick, A. 1987 Interacting boundary layers. *Z. Angew. Math. Mech.* **67**, T3–T13.

Kluwick, A. 1991 Small-amplitude finite-rate waves in fluids having positive and negative nonlinearity. In *Nonlinear waves in real fluids* (ed. A. Kluwick), pp. 1–43. Springer.

Kluwick, A. 1993 Transonic nozzle flow of dense gases. *J. Fluid Mech.* **247**, 661–688.

Kluwick, A. 1994 Interacting laminar boundary layers of dense gases. *Acta Mechanica* (Suppl. 4), pp. 335–349.

Kluwick, A. & Reiterer, M. 1998 On three-dimensional marginal separation. *Z. Angew. Math. Mech.* **78** (Suppl. 2), 543–544.

Kluwick, A. & Zieher, F. 2001 Linearly retarded dense gas boundary layer flows over a flat plate. (In preparation.)

Kluwick, A., Gittler, Ph. & Bodonyi, R. J. 1984 Viscous–inviscid interactions on axisymmetric bodies of revolution in supersonic flow. *J. Fluid Mech.* **140**, 281–301.

Kluwick, A., Reiterer, M. & Hackmüller, G. 1997 Marginal separation caused by three-dimensional surface mounted obstacles. In *Proc. 2nd Int. Conf. on Asymptotics in Mechanics, St Petersburg, 1996*, pp. 113–120.

Oswatitsch, K. 1958 Die Ablösebedingungen von Grenzschichten. In *Grenzschichtforschung, IUTAM Symp., Freiburg, 1957* (ed. H. Görtler), pp. 357–367. Springer.

Park, S.-H. 1994 Viscous–inviscid interactions of dense gases. PhD thesis, Virginia Polytechnic Institute and State University.

Prandtl, L. 1938 Zur Berechnung der Grenzschichten. *Z. Angew. Math. Mech.* **18**, 77–82.

Reiterer, M. 1998 Dreidimensionale marginale Ablösung. PhD thesis, Vienna University of Technology.

Ruban, A. I. 1981*a* Singular solution of boundary-layer equations that can be extended continously through the point of zero surface friction. *Izv. Akad. Nauk SSSR: Mekh. Zhidk. Gaza* **6**, 42–52.

Ruban, A. I. 1981*b* Asymptotic theory of short separation regions on the leading edge of a slender airfoil. *Izv. Akad. Nauk SSSR: Mekh. Zhidk. Gaza* **1**, 42–51.

Smith, F. T. 1982 On the high Reynolds number theory of laminar flows. *IMA J. Appl. Math.* **28**, 207–281.

Smith, F. T., Sykes, R. I. & Brighton, P. W. M. 1977 A two-dimensional boundary layer encountering a three-dimensional hump. *J. Fluid Mech.* **83**, 163–176.

Stewartson, K. 1962 The behaviour of a laminar compressible boundary layer near a point of zero skin friction. *J. Fluid Mech.* **12**, 117–128.

Stewartson, K. & Williams, P. G. 1969 Self-induced separation. *Proc. R. Soc. Lond.* A **312**, 181–206.

Stewartson, K., Smith, F. T. & Kaups, K. 1982 Marginal separation. *Stud. Appl. Math.* **67**, 45–61.

Thompson, P. A. 1991 Liquid–vapor adiabatic phase changes and related phenomena. In *Nonlinear waves in real fluids* (ed. A. Kluwick), pp. 147–214. Springer.

Thompson, P. A. & Lambrakis, K. C. 1973 Negative shock waves. *J. Fluid Mech.* **60**, 187–208.

Wang, K. C. 1971 On the determination of zones of influence and dependence for three-dimensional boundary-layer equations. *J. Fluid Mech.* **48**, 397–404.

Zametaev, V. B. 1989 Formation of singularities in a three-dimensional boundary layer. *Izv. Akad. Nauk SSSR: Mekh. Zhidk. Gaza*, 58–64.

Zel'dovich, Ya. B. 1946 On the possibility of rarefaction shock waves. *Zh. Eksp. Teor. Fiz.* **4**, 363–364.

PHILOSOPHICAL TRANSACTIONS OF THE ROYAL SOCIETY A MATHEMATICAL, PHYSICAL & ENGINEERING SCIENCES